HHS Public Access

Author manuscript

Langmuir. Author manuscript; available in PMC 2019 March 15.

Published in final edited form as:

Langmuir. 2017 March 28; 33(12): 3018–3027. doi:10.1021/acs.langmuir.6b04400.

Addition of Fluorescence Lifetime Spectroscopy to the Tool Kit Used to Study the Formation and Degradation of Luminescent Quantum Dots in Solution

Taeyjuana Y. Lyons, **Denise N. Williams**, and **Zeev Rosenzweig***

Department of Chemistry and Biochemistry, University of Maryland Baltimore County, Baltimore, Maryland 21250, United States

Abstract

The increasing commercialization of consumer electronic products that make use of II–VI semiconductor quantum dots (QDs) has raised significant concerns about their impact on natural systems and human health once they are released into the environment at the end of the product's lifetime. In this paper, we demonstrate the addition of fluorescence lifetime spectroscopy to the existing tool kit of spectroscopic techniques to quantitatively monitor changes in QD properties as they form and degrade in solution. Our study reveals that because of its rich information content, fluorescence lifetime spectroscopy has a limited utility as a stand-alone technique in the study of QD formation and degradation. However, combining fluorescence lifetime spectroscopy with the commonly used emission quantum yield and peak width measurements along with other analytical methods, including ultraviolet–visible spectroscopy, transmission electron microscopy, and inductively coupled plasma mass spectrometry measurements, significantly enhances the existing analytical tool kit and provides the capability to monitor in real time, the formation and degradation of luminescent QDs in organic and aqueous solutions under environmentally relevant conditions.

Graphical Abstract

*Corresponding Author: zrosenzw@umbc.edu.

Supporting Information

The Supporting Information is available free of charge on the ACS Publications website at DOI: 10.1021/acs.langmuir.6b04400. Normalized absorbance spectra of QDs during crystal growth, TEM images of CdSe QDs that were prepared using rapid and slow synthesis techniques, STEM image of 2.4 nm CdSe QDs, EDX graph, screenshot of the output from Felix GX fitting software, and summary of the average fluorescence lifetime and fluorescence lifetime components for all lifetime traces discussed in the paper (PDF)

The authors declare no competing financial interest.

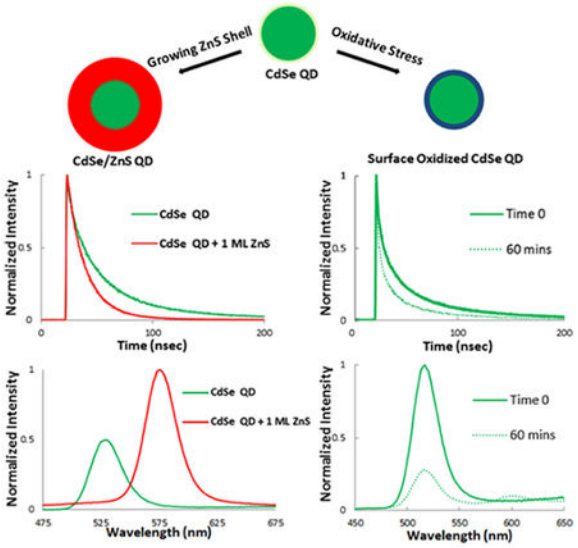

INTRODUCTION

Luminescent semiconductor quantum dots (QDs) exhibit unique size-dependent luminescence properties due to quantum confinement effects.[1] II–VI luminescent semiconductor QDs, for example, CdSe QDs absorb broadly and emit size-tunable visible light when excited using an ultraviolet (UV) excitation source.[2] The wide range of potential applications of luminescent QDs has spurred considerable research efforts to develop reliable QD synthesis and characterization techniques.[3,4] Since its development in the early 1990s, the hot injection method has served as the gold standard for QD synthesis.[5] Yet, researchers are constantly looking to develop new and more green synthesis techniques that match the ability of the hot injection method to yield high-quality QDs.[6]

Luminescent QDs are used in bioimaging and biosensing applications.[6–12] In ours, and in other laboratories, QD-based fluorescence resonance energy transfer (FRET) probes were developed and used in biological and cellular assays.[13–18] More recently, luminescent QDs have been incorporated into mass produced consumer electronic products, for example, QD TVs[19] and were proposed as optical absorbers and charge carriers in photovoltaic devices.[20] The adaptation of luminescent QDs in such wide-range applications raises significant concerns about their long-term chemical stability. The poor chemical stability of luminescent QDs would not only affect their luminescence properties but also increase their environmental and human health impact because of the release of potentially toxic degradation products.

A broad tool kit of analytical techniques is required to fully characterize semiconductor QDs, and there is no single technique that has the capability to fully characterize the QD properties alone. Ultraviolet–visible (UV–Vis) and fluorescence spectroscopies, transmission electron microscopy (TEM), dynamic light scattering (DLS), Fourier transform infrared spectroscopy (FTIR), X-ray diffraction, and X-ray photoelectron spectroscopy (XPS) are often used for QD characterization.[21–23] Among these techniques, UV–Vis and

steady-state fluorescence spectroscopies are the only ones that have the capability to provide real-time monitoring of QD formation and degradation. However, both techniques are concentration-dependent, and UV–Vis spectroscopy often lacks sufficient sensitivity to reveal QD degradation. Changes in the fluorescence peak shape, peak width, and emission quantum yield (QY) are observed during QD growth and degradation, but these techniques do not discriminate between bulk structural defects, surface defects, and surface traps, which induce nonradiative pathways and decrease the rate of radiative electron–hole recombination processes. Time-correlated single photon counting (TCSPC) fluorescence lifetime spectroscopy could offer an additional insight into the QD luminescence properties during growth and degradation, particularly when the technique is combined with existing techniques. Fluorescence lifetime spectroscopy was previously used to characterize luminescent QDs in aqueous solutions and biological systems.[24–29] For example, Mulvaney and co-workers established a direct link between the shell thickness in core/shell QDs and their emission QY and fluorescence lifetime.[28,29]

This paper uniquely focuses on investigating the utility of fluorescence lifetime spectroscopy in studying the growth of core and core/shell QDs, their surface modification to enable their aqueous solubility and their degradation under conditions of elevated temperature in organic solvents and under conditions of oxidative stress in aqueous solution. This paper reveals the multiple factors that affect the fluorescence lifetime and provides additional insights into the parameters that affect the luminescence properties of semiconductor QDs. Undoubtedly, because of the inherent complexity of luminescent QDs, more sophisticated time-resolved photoluminescence measurements, for example, at a low temperature and on a single QD, are necessary to better understand the photodynamic properties of luminescent QDs, including their fluorescence lifetime traces. Yet, the study demonstrates that fluorescence lifetime spectroscopy of QD samples under ambient conditions, when combined with complementary techniques, increases our understanding of the impact of reaction and environmental conditions and surface properties on the QD luminescence properties as they grow and degrade in solution. Fluorescence lifetime measurements reveal that common assumptions, for example, about the ability to synthesize high-quality luminescent QDs with a wide size range, using a single semiconductor material, has its limits. Our study shows that overly small QDs are dominated by nonradiative transitions, whereas overly large QDs are dominated by complex photodynamics that often leads to delayed emission or a long fluorescence lifetime, with significant deviations from monoexponential decay fit functions. Both phenomena lead to reduced emission QY. Fluorescence lifetime measurements also provide a clearer answer about the coating thickness needed to passivate luminescent QDs and protect them from chemical degradation. Our study shows that adding relatively simple fluorescence lifetime measurements to the tool kit of analytical methods used to characterize luminescent QDs during formation and degradation results in new information necessary to synthesize QDs that are characterized with superb luminescence properties and high chemical stability.

MATERIALS AND METHODS

Reagents.

Selenium (Se, 99.99%), trioctylphosphine (TOP, 97%), trioctylphosphine oxide (TOPO, 99%), cadmium acetylacetonate(99.9%), tetradecylphosphonic acid (97%), fluorescein sodium salt (BioReagent Grade), 1-octadecene (90%), hexamethyldisilathiane [$(TMS)_2S$, synthesis grade], diisooctylphosphinic acid (90%), methane sulfonyl chloride (99.9%), triethylamine (99%), sodium bicarbonate (99.7%), sodium azide (99.5%), triphenylphosphine (99%), (±)-α-lipoic acid (thioctic acid, 99%), 4-(dimethylamino)-pyridine (DMAP, 99%), dicyclohexylcarbodiimide (DCC, 99%), sodium borohydride (99%), Celite 577 (fine), and silica gel 60 Å (230–400 mesh) were purchased from Sigma-Aldrich. Zinc formate (98%) and 1-dodecylphosphonic acid (DPA, 95%) were purchased from Alfa Aesar. Poly(ethylene glycol)methyl ether (average M_W 750) was purchased from Acros Organic. Hydrogen peroxide (10%), 1-hexadecylamine (HDA, 90%), oleylamine (C18 content 80–90%), nitric acid (TraceMetal Grade), hydrochloric acid (37.1%), anhydrous sodium sulfate (100%), and all solvents were purchased from Acros Organics or Fisher Scientific. An Instrument Calibration Standard 2 (5% HNO_3/Tr. Tart. acid/Tr. HF) for inductively coupled plasma mass spectrometry (ICP-MS) was purchased from Claritas PPT SPEX CertiPrep. All chemicals were used as received.

UV–Vis, Steady-State Fluorescence, and Fluorescence Lifetime Spectroscopies.

UV–Vis absorbance measurements were completed using a Thermo Scientific Evolution 201 UV–Vis spectrophotometer. All steady-state and fluorescence lifetime measurements were carried out using a PTI-Horiba QuantaMaster 400 with a PicoMaster TCSPC steady-state and fluorescence lifetime spectrometer. A 75 watt xenon lamp was the excitation source for all steady-state photoluminescence measurements. A 375 nm femtosecond pulsed laser diode, operated at 1 MHz, was the excitation source for all QD fluorescence lifetime measurements. The analysis of all fluorescence spectra and lifetime traces was completed using the PTI-Horiba Felix-GX software.

High-Resolution TEM.

A high-resolution Titan 80–300 analytical transmission electron microscope was used to image the luminescent QDs using accelerating voltages in the range of 80–300 kV in both the transmission and scanning modes. The Titan TEM is equipped with an energy-dispersive X-ray spectroscopy (EDX) module, which was used to measure the atomic composition of the luminescent QDs. Samples were prepared by purifying a small amount of the QD solution at micromolar levels and drop-casting 10 μL of the solution onto 400 mesh, copper grids with an ultrathin carbon film on a holey carbon support film (Ted Pella, Inc.). The grids were then placed in a vacuum oven overnight before being inserted into the transmission electron microscope.

ICP-MS.

ICP-MS measurements of QDs and QD filtrates were carried out using a PerkinElmer NexION 300D single quad mass spectrometer. An instrument calibration standard 2 (5%

HNO_3/Tr. Tart. acid/Tr. HF) was used to calibrate the instrument between 1 ppb and 1 ppm. The QD samples were prepared by adding 15 μL of 1 μM QD samples to 185 μL of 6 M nitric acid solution. The QD solution was kept under these conditions overnight and then diluted using Millipore water to a total volume of 10 mL to decrease the nitric acid level to less than 5% immediately before instrument loading.

Synthesis of CdSe QDs Using a Rapid Synthesis Method.

A rapid synthesis of CdSe QDs was carried out following a previously reported well-established protocol.[29] A selenium precursor solution was prepared by adding Se (0.332 g, 4.20 mmol) to TOP (5 mL) in a 20 mL scintillation vial. The vial was sealed, and the mixture was heated to 80 °C and sonicated using a bath sonicator to dissolve Se. The mixture was then degassed under vacuum for 30 min and backfilled with nitrogen gas. A mixture of HDA (5.0 g, 20.7 mmol), cadmium acetylacetonate (0.311 g, 1.0 mmol), tetradecylphosphonic acid (0.585 g, 2.1 mmol), and TOP (10 mL) was added to a 50 mL three-necked round-bottom flask and sealed with a septum. The mixture was heated to 100 °C and degassed under vacuum for 30 min. The flask was backfilled with nitrogen gas, then heated to 250 °C, and maintained at this temperature for 30 min under reflux conditions. The mixture was cooled down to 100 °C and then degassed under vacuum for the final time. The flask was backfilled with nitrogen gas and heated to 300 °C. The Se precursor solution was injected rapidly at 300 °C, and the reaction mixture was kept at this temperature. Small aliquots of the solution were taken out at various time intervals to realize the desired CdSe QD diameter. The solutions were all annealed overnight at 50 °C. 1-Butanol was added to each of the solutions before they were spun at 3200 rpm at room temperature. Excess amounts of 50:50 mixture of acetone and methanol were then added to the solutions to cause the QDs to flocculate. The solutions were spun for additional 5 min at 3800 rpm. The supernatant was discarded, and the QD-containing pellet was dissolved in 1–2 mL of toluene. The purification process was repeated two more times.

Synthesis of CdSe QDs Using a Slow Synthesis Method.

A slower synthesis of CdSe QDs was realized by modifying the synthesis protocol described above by changing the ratio between the reactants and by using a 16-carbon diisooctyphosphonic acid versus the 14-carbon tetradecylphosphonic acid that was used in the rapid QD synthesis. A selenium precursor solution was prepared by adding Se (0.351 g, 4.4 mmol) to TOP (4.0 mL) in a 20 mL scintillation vial. The vial was sealed, and the mixture was heated to 80 °C and sonicated using a bath sonicator to dissolve selenium. The solution was then degassed under vacuum for 30 min and backfilled with nitrogen gas. A mixture of TOPO (2.0 g, 5.2 mmol), HDA (8.0 g, 33.1 mmol), TOP (10 mL), cadmium acetylacetonate (0.311 g, 1.0 mmol), and diisooctylphosphinic acid (0.76 mL) was added to a 50 mL three-necked round-bottom flask. The mixture was heated to 100 °C, degassed under vacuum to remove water and oxygen, and backfilled with nitrogen gas. The solution was then heated to 320 °C under reflux conditions. The Se solution was rapidly injected into the reaction mixture, which was then cooled and kept at 270 °C to allow the QD growth. Small aliquots of the solution were taken out at various time intervals to realize the desired QD diameter. The collected QD solutions were all annealed overnight at 50 °C. The resultant

QDs were purified by the same method that was used to purify the smaller and more rapidly formed QDs described above.

Synthesis of CdSe/ZnS Core/shell QDs.

The CdSe QDs were coated with a ZnS shell using a successive ionic layer adsorption and reaction (SILAR) method, a chemical method that is used to form uniform and large area thin films.[30] It is based on the immersion of QDs in separate solutions containing zinc cations and sulfide anions.2.4 nm CdSe QDs (0.3 μmol) were purified and dissolved at 100 °C in a mixture of 6 mL 1-octadecene, 6 mL oleylamine, 4 mL of TOP, and 10 mg DPA in a three-neck round bottom flask. The mixture was degassed under vacuum for 30 min, until bubbling stopped, to remove water and oxygen. The flask was then backfilled with nitrogen gas. The solution was heated to 160 °C under reflux conditions, and the Zn precursor solution (0.05 M zinc formate in oleylamine) was slowly added to the solution over a period of 15 min using a syringe pump. The sulfur precursor [0.25 M $(TMS)_2S$ in TOP] was subsequently added to the solution over a period of 15 min using a syringe pump. The reaction mixture was kept under these conditions for 30 min to allow the formation and annealing of the ZnS monolayer. The temperature was increased to 170 °C, and the process was repeated to add a second and then a third monolayer shell. The temperature was increased by 10 °C for each added monolayer shell.

Surface Modification of CdSe/ZnS QDs for Aqueous Solubility.

Two surface modification techniques were used to enable the aqueous solubility of the QDs. First, purified hydrophobic CdSe/ZnS QDs were rendered water soluble by exchanging native ligands (fatty acids/TOP) with dihydrolipoic–poly(ethylene glycol)-monomethyl ether (DHLA-PEG750-OCH3). These ligands were synthesized by coupling modified PEG (M_W 750 g/mol) to thioctic acid via an amide conjugation reaction, following a synthesis protocol previously described by Mei et al.[31,32] This ligand synthesis strategy yields strongly coordinated, acid/base stable, and compact water-soluble QDs, ideally suited for long-duration studies under diverse conditions. The ligand coating of the QDs followed the protocol of Liu and Snee.[33] Alternatively, the QDs were coated using bovine serum albumin (BSA). This was realized by first adding excess acetone to 5 mL of 5 μM QDs dissolved in hexane. The QDs were precipitated using slow-speed centrifugation of 3800 rpm for 5 min. The supernatant was discarded. The QDs were redispersed in 1 mL of chloroform and then vacuumed out to form a thin layer of QDs at the bottom of the vial. Five mL of 0.1% BSA in 10 mM phosphate buffer (pH 7.4) was added to the QD-containing vial. The solution was vortexed for two minutes and sonicated for 90 min to realize a homogeneous QD suspension. An ice-water bath was used to ensure that the QD solution was not heated during the sonication. The resultant mixture was cloudy due to QD aggregation, but the QDs maintained their emission properties including high emission QY and narrow and symmetric emission peaks.

QD Characterization.

The concentration and initial sizing of the CdSe QDs were determined using the absorbance spectra based on a previously published work.[2] The average size, shape, crystallinity, and elemental composition of the QDs were confirmed using a high-resolution transmission

electron microscope, which is equipped with Energy-Dispersive X-ray spectroscopy (EDX) capabilities. The atomic contents of CdSe and CdSe/ZnS QDs were quantitatively determined using inductive coupled plasma mass spectrometry (ICP-MS). The emission peak and the full width at half-maximum (FWHM) values were measured using the PTI-Horiba Felix-GX software. The QY values of the QDs were calculated based on a previously published method.[3] Fluorescein sodium salt dissolved in 10 mM phosphate buffer was used as the standard for the QY measurements.[4] Fluorescence lifetime traces of the QDs were analyzed using the PowerFit-10 multiexponential fitting algorithm of PTI-Horiba Felix-GX software. All QD lifetime traces were fitted using the following equation

$$I(t) = a_1 \exp\left(-t/\tau_1\right) + a_2 \exp\left(-t/\tau_2\right) + a_3 \exp\left(-t/\tau_3\right) + a_4 \exp(-t/\tau 4)$$

The QD fluorescence lifetime (τ) was calculated as the weighted average of the lifetime components (τ_1, τ_2, τ_3, and τ_4), where the a_1, a_2, a_3, and a_4 values indicate the weights of τ_1, τ_2, τ_3, and τ_4, respectively. The fitting parameter χ^2 was used to determine the quality of the fit; fits with corresponding values of χ^2 between −0.1 and 0.1 were considered acceptable. All fluorescence lifetime data were taken in triplicate, and the standard errors were extracted from the fit values.

RESULTS AND DISCUSSION

Monitoring the Formation of CdSe QDs.

Our studies focused on monitoring the growth of CdSe QDs ranging in diameter between 1.8 and 3.2 nm, using the rapid hot injection method (see Materials and Methods for details). The lower and upper limits of the CdSe QD diameters were 1.8 and 3.2 nm when the QD were prepared using this method. The current spectroscopy-based tool kit used to monitor and assess the luminescence properties of the luminescent QDs during synthesis includes UV–Vis and fluorescence techniques, which determine the emission peak wavelength, peak width, and emission QY. The addition of fluorescence lifetime spectroscopy to the tool kit enables the study of QD luminescence properties more quantitatively as the QD form or degrade. This is because fluorescence lifetime spectroscopy is highly sensitive to the crystalline quality of the QDs when they form and to the QD surface properties and their interactions with the environment, which affect their crystalline quality, during chemical degradation. Additionally, the concentration dependence of the QD fluorescence lifetime is weak, particularly when limiting their concentration to minimize collision-driven luminescence quenching. We anticipated difficulties in interpreting the fluorescence lifetime results as the QDs grew because of the simultaneous changes in the QD size and the emission peak wavelength, in the crystalline quality of the QDs, which improves with a longer reaction and annealing times, and in the QD size distribution, which is expected to broaden with longer reaction times because of simultaneous Ostwald ripening of existing nanocrystals and nucleation and growth of new crystals. Additionally, fluorescence lifetime spectroscopy measurements of QD solutions at room temperature do not discriminate between homogeneous effects, for example, QDs exhibiting multiple dynamics, and heterogeneous effects, which are averaged out in solution. The fluorescence lifetime traces of samples taken from the reaction mixture at various time intervals, which contain

luminescent QDs of increasing diameters, are shown in Figure 1A. The excitation wavelength was 375 nm, and the emission wavelength was set at the maximum emission peak intensity, which varies with increasing QD diameter. The complex nature of the QD photodynamic properties is evident by the fact that a four-term multiexponential fit function is necessary to describe the fluorescence lifetime traces of the formed QDs. Although the weighted fluorescence lifetime is an average value, it still provides important insights into the growth and crystalline quality of the QDs during formation. The size dependence of the fluorescence lifetime is shown in Figure 1B. The size dependence of the QD emission QY and the representative emission peaks of QDs of various diameters are shown in Figure 1C,D, respectively. For CdSe QDs prepared using the rapid synthesis technique, the fluorescence lifetimes range widely from 5.6 ± 2.0 ns (Figure 1A, 1.8 nm QD, blue) to 24.6 ± 0.1 ns (Figure 1A, 3.2 nm QD, green). The fluorescence lifetime first increases when the QD diameter increases from 1.8 nm (1A, blue) to 2.4 nm (1A, black); then, it varies slightly when the QD diameter increases from 2.4 to 2.8 nm (1A, red) and increases again when the QD diameter increases from 2.8 to 3.2 nm (1A, green). An overall increase in the fluorescence lifetime with the QD diameter is expected because of a decrease in quantum confinement as the QDs grow. However, the observed nonmonotonic increase and the correlating size dependence of the emission QY (Figure 1C) suggest that the rapid synthesis technique yields high quality QDs in a narrow size range around 2.4 nm where the fluorescence lifetime stabilizes and the emission QY reaches a maximum of 30%. The corresponding increase in the fluorescence lifetime and the emission QY in the size range of 1.8–2.4 nm might be attributed to an improvement in the crystalline quality as the QDs grow. The fluorescence lifetime and the emission QY decrease slightly and remain around 20 ns and 25%, respectively, in the QD size range of 2.4–2.8 nm. The slight decrease in both the QD fluorescence lifetime and the emission QY might be due to an increase in the rate of nonradiative electron–hole recombination due to the formation of crystalline defects. The QD crystal growth from 2.8 to 3.2 nm results in an increase in the fluorescence lifetime to 24.6 ±0.2 ns, whereas the emission QY continues to decrease down to 5%. The increase in the QD fluorescence lifetime while the emission QY continues to decline might be explained by the appearance of defects that slow down the rate of radiative electron–hole recombination. We also investigated the deviation of the fit function of the fluorescence lifetime from a monoexponential fit function as the QDs grow. Interestingly, the deviation from a monoexponential fit increases with increasing QD diameters. For the smallest size QD of 1.8 nm, the accumulative weight of higher-order exponential terms is 36%. It increases to 70% as the QDs grow, with t_4 values of around 100 ns, increasing in weights from 0.1 to 8%. At the same time, the QD fluorescence lifetime and the emission QY increase, as their crystalline quality improves due to longer reaction times. The magnitude of the deviation from the monoexponential fit depends on a combination of homogeneous and heterogeneous contributions that are difficult to discern at room temperature. A significant contribution to the nonexponential decay of luminescent QDs at room temperature is caused by the exciton singlet–triplet splitting and the thermal activation of the triplet states, which results in delayed emission from the singlet states. The effect of singlet–triplet splitting and the thermal activation of the triplet states increase with the QD diameter because the singlet–triplet splitting is smaller for larger QDs. This results in an increasing deviation from the monoexponential decay with increasing QD size. In addition, longer reaction times to yield

larger luminescent QDs result in a broader QD size distribution, which also contributes to a larger deviation of the fluorescence lifetime from mono-exponential decay. The increased deviation of the QD fluorescence lifetime from a monoexponential fit function with increasing QD size suggests that this deviation depends more strongly on the rate of singlet–triplet splitting, the QD size distribution, and the QD crystalline quality that improves with longer reaction times. We therefore concluded that the deviation of the QD fluorescence lifetime from a mono-exponential fit function could only be used as a determinant of QD crystalline quality when the QD diameter and size distribution are near constant. The QD emission peaks shown in Figure 1D reveal that the emission spectrum of the smallest size QD (1.8 nm, blue) has a red-shifted peak in addition to the QD excitonic emission peak at 460 nm. The red-shifted broad peak is attributed to crystalline defects that form because of the short reaction time used to synthesize small size QDs. The excitonic emission peaks of the QDs are red-shifted with increasing diameter (2.4 nm, λ = 520 nm; 2.8 nm, λ = 540 nm; and 3.2 nm, λ = 560 nm), but the peak FWHM values of the QDs remain largely unchanged at approximately 35 nm, as their diameter increases from 2.4 to 3.2 nm. This means that the distribution of bandgap energies of the QDs in fact narrows from 2.38 eV (520 nm) to 2.21 eV (560 nm), likely due to narrowing the QD size distribution as the QD grow in this size range. Further growth of the QDs would lead to broader emission peaks because of a greater QD size distribution. The complex size dependence of the QD luminescence properties suggests that an entire tool kit of fluorescence measurements is needed to fully characterize their properties. The QD fluorescence lifetime and the emission QY depend strongly on the QD diameter and the crystalline quality. The fluorescence lifetime also depends on the QD size distribution. The emission peak shape and width depend strongly on the crystalline quality and the size distribution, whereas the emission peak wavelength depends strongly on the QD size. The size dependence of the QD fluorescence lifetime is more complex because it contains more information about the type of QD defects and the affected electronic transitions, radiative versus nonradiative. It is fair to conclude that QD fluorescence lifetime measurements would be easier to interpret and therefore more informative in samples where the QD size and the size distribution remain largely unchanged throughout the measurements. As will be seen in the next section, the synthesis conditions play a significant role in realizing QDs with a desirable size and a narrow size distribution.

Impact of Synthesis Conditions on QD Luminescence Properties.

This section focuses on the impact of QD synthesis reaction conditions on their luminescence properties. Figure 2 shows a comparison between the emission peaks (Figure 2A) and the fluorescence lifetime traces (Figure 2B) of 3.2 nm CdSe QDs, which were prepared using the rapid and slow synthesis methods (see Materials and Methods). The peak width (FWHM) of CdSe QDs, which were prepared using the rapid synthesis method is narrower and more symmetric (35 nm, Figure 2A, black) than the same properties of CdSe QDs, which were prepared using the slow synthesis method (45 nm, Figure 2A, red). The impact of synthesis conditions on the QD fluorescence lifetime is even more profound. The fluorescence lifetime of the QDs that were prepared using the slow synthesis method is 8.8 ± 0.3 ns (Figure 2B, red), whereas the fluorescence lifetime of the QDs that were prepared using the rapid synthesis method is significantly longer at 25.7 ± 0.8 ns (Figure 2B, black). In addition, the deviation of the fluorescence lifetime from monoexponential decay fit is

larger for QDs that were prepared using the rapid synthesis method. The accumulative weight of higher exponential terms for the rapidly formed QDs is 62%. It decreases to 41% for the same size QDs that were prepared using the slow synthesis method. It is fair to conclude that a longer reaction time leads to improvement in the crystalline quality because of a longer annealing time. A longer reaction time leads to a higher emission QY (40% as opposed to 18%), a shorter fluorescence lifetime, and a smaller deviation of the fluorescence lifetime from monoexponential decay fit. This is due to a decrease in the density and the impact of defects and surface traps, which slow down the radiative electron–hole recombination processes. On the other hand, longer reaction times result in a broader QD size distribution and hence broader emission peaks.

Monitoring the Formation of Core/Shell CdSe/ZnS QDs.

CdSe QDs are often coated with a higher bandgap and crystal plane matching material, such as ZnS, to form CdSe/ZnS core/shell QDs. The shell is used to passivate the QD core surface, which results in a higher chemical stability and superior luminescence properties. Coating QD cores with a shell leads to an emission peak red shift and an increase in the emission QY. We investigated the impact of coating CdSe QDs with a ZnS shell on the fluorescence lifetime of the resultant core/shell QDs. CdSe QD (3.0 nm) were coated with one monolayer shell at a time, using the SILAR method (see Materials and Methods). Figure 3 illustrates the QD fluorescence lifetime as monolayers of ZnS are added to form the core–shell structure. In our laboratory, which primarily focuses on the development and application of luminescent QDs in bioimaging and biosensing applications, we use a shell thickness of three monolayers because this shell thickness yields the highest emission QY and chemical stability in solution, with minimal broadening of the QD emission peak. The QD fluorescence lifetime decreases from 29.1 ± 1.4 to 17.9 ± 1.1 ns after the first ZnS monolayer is formed on the CdSe QDs. The fluorescence lifetime stabilizes with the addition of two additional monolayers. The emission QY increases from 23 to 51% when the CdSe QDs are coated with one ZnS monolayer and further increases to 62% when coated with three ZnS monolayers and remains constant with a further increase in shell thickness. The significant decrease in the fluorescence lifetime and the corresponding increase in the emission QY demonstrate that, as expected, the formation of the shell passivates the surface of the CdSe QD cores and decreases the impact of surface defects and traps, which slow the rate of radiative electron–hole recombination processes. The fluorescence lifetime results indicate that most of the passivation effect is realized by coating the CdSe QDs with a single monolayer shell, although additional improvement in the emission QY is obtained by adding two monolayers of ZnS shell. These results suggest that for applications of CdSe/ZnS QDs in consumer electronics such as tablets and TVs, in which the QDs are embedded in a protective polymer film and shielded from the environment by being placed behind glass, it may be sufficient to coat the QDs with only a single monolayer of ZnS shell to improve their luminescence properties. Additional coating thickness would only limit the QD density and the overall film brightness without providing a significant level of additional passivation. A recent study by Vanmaekelbergh and co-workers[34] revealed a significant increase in delayed emission in core–shell luminescent QDs with increasing shell thickness. A long lifetime component on the microsecond time scale, which contributes a weight of up to 20% to the QD fluorescence lifetime fit function, was observed as the ZnS shell thickness increased to

12 monolayers. Although our study focused on a thin ZnS shell of up to three monolayers, we also observed long lifetime components (τ_4) in the multiexponential fit function of up to 500 ns in our CdSe/ZnS core–shell QDs. However, because of the thin ZnS shell, the weights of these long lifetime components are limited, typically between 1 and 2%. It is reasonable to assume that QD-delayed emission would play a more significant role in bioimaging applications that require thicker protective shells to ensure high QD chemical stability in complex biological environments. Whereas this section focuses on the sensitivity of fluorescence lifetime spectroscopy to changes in the shell thickness, the next section focuses on the impact of QD surface chemistry and solvent on their fluorescence lifetime.

Impact of Surface Chemistry and Solvent on the Fluorescence Lifetime of CdSe and CdSe/ZnS QDs.

It is expected that the surface chemistry and the chemical environment of luminescent QDs would affect their luminescence properties including their fluorescence lifetime. Figure 4 illustrates the impact of various surface chemistries and solvents, hydrophobic versus hydrophilic, on the fluorescence lifetime of CdSe/ZnS QDs (2.4 nm CdSe QDs with three monolayers ZnS shell) capped with TOPO ligands in chloroform (blue), CdSe/ZnS QDs capped with DHLA–PEG molecular ligands (green), and CdSe/ZnS QDs capped with BSA in 10 mM phosphate buffer at pH 7.2 (red). As previously mentioned, the fluorescence lifetime traces of CdSe/ZnS QDs are complex and are therefore described using multiexponential fit functions with as many as four exponential components. Yet, the weighted fluorescence lifetime and the deviation of the fluorescence lifetime from monoexponential decay fit function provide important insights into the role of surface chemistry on the QD luminescence properties. The weighted fluorescence lifetime decreases from 18.7 ± 1.8 ns for TOPO-capped CdSe/ZnS QDs in chloroform to 9.6 ± 0.4 ns for CdSe/ZnS capped with DHLA-PEG750-OCH3 molecular ligands and to 7.8 ± 0.8 ns for CdSe/ZnS QDs coated with BSA. A significant decrease in the emission QY from 60 to 18% and 22% is observed when the QDs are coated with the hydrophilic DHLA-PEG750-OCH_3 ligands and BSA. The corresponding decrease in the fluorescence lifetime and the emission QY is indicative of stronger interactions of the QDs with water molecules, which lead to a higher rate of nonradiative electron–hole recombination processes. The fluorescence lifetimes of CdSe and CdSe/ZnS QDs in chloroform and aqueous buffers with DHLA-PEG750-OCH_3 and BSA coating remained largely unchanged during a 3 week observation period. This indicates that the surface modification of CdSe/ZnS QDs with molecular ligands or protein coating results in highly stable QDs that maintain their luminescence properties in aqueous solution. It should be noted, however, that a more detailed analysis of the fluorescence lifetime of DHLA-PEG750-OCH_3 and BSA-capped QDs reveals an important difference. The most rapid component of the multiexponential function τ_1 of DHLA-PEG750-OCH_3-capped QDs is 13.0 ± 0.75 ns, and the component weight is 44%. These values are slightly reduced from the values obtained for TOPO-capped QDs in chloroform, where τ_1 = 15.6 ± 1.65 ns, and the component weight is 51%. On the other hand, a much more rapid lifetime component τ_1 = 0.34 ± 0.07 ns (within the sensitivity of our TCSPC instrument) and a component weight of 53% is observed in BSA-capped QDs. The appearance of such a rapid lifetime component in the BSA-capped QDs suggests that the formation of QD aggregates provides a rapid radiative pathway, which negates the

impact of QD surface traps that are more accessible to water molecules, and increases the fluorescence lifetime. The slightly higher emission QY for BSA-capped QDs than that for QDs capped with molecular ligands suggests that QD aggregation does not provide nonradiative pathways that would lower the emission QY. The ability to use the rapid lifetime component to assess the aggregation state of luminescent QDs is of great potential importance and is currently explored in our laboratory.

Degradation of CdSe QDs in Organic Solvents under Conditions of Elevated Temperature.

We investigated the chemical stability of CdSe QDs under conditions of elevated temperature. A solution of 5 mL of 1 μM CdSe QDs in chloroform was heated to 60 °C using an oil-bath for 60 min. A small aliquot of the sample was taken out every 10 min and cooled to room temperature; the emission spectra and the fluorescence lifetime traces were measured. Figure 5a shows the normalized QD fluorescence spectra under conditions of elevated temperature. Figure 5b shows the fluorescence lifetime traces of the QDs right before heating and at 20 min intervals up to 60 min. Dramatic decreases in the emission QY from 21 to 4% and in the weighted average fluorescence lifetime of the QDs from 19.2 ± 0.4 to 6.1 ± 0.1 ns are observed, which is indicative of QD degradation. This conclusion is supported by the increased monoexponential character of the fluorescence lifetime, as complex radiative transitions that lengthen the fluorescence lifetime are silenced, giving way to nonradiative transitions. The emergence of an additional broad peak centered at 600 nm in the steady-state fluorescence spectrum, most likely due to surface trap emission from the degraded QDs, further supports our conclusion that the CdSe QDs degrade under conditions of elevated temperature. While being carried out in chloroform, rapid thermal degradation of CdSe QDs at 60 °C is a source of concern for the utility of luminescent QDs in solid-state devices such as TVs and cell phones, which easily reach this and even higher temperatures during operation. Similar concerns were raised in a previous study by Law and co-workers who evaluated the photothermal stability of PbS QDs in solid-state devices and found that PbS QD-containing films degrade under conditions of elevated temperature of 85 °C because of oxidation, ripening, and sintering.[35] This stresses that care must be given to protect the QDs from thermal degradation by efficient heat dissipation.

Monitoring the Degradation of CdSe QDs in Aqueous Solution.

The chemical stability of water-soluble QDs under environmentally relevant conditions is important when considering their potential impact on human health and the environment. It is more likely that QDs will appear in the environment in the form of aggregates or encased in a polymer matrix rather than in a pristine, monodispersed form. It should be noted that CdSe/ZnS QDs are synthesized in organic solvents and the resultant QDs are capped with TOPO ligands. A ligand-exchange process must be carried out to render the QDs miscible in aqueous solution. In our studies, both types of aqueous QDs, monodispersed QDs capped with molecular ligands and aggregated QDs capped with BSA, were exposed to0.75% hydrogen peroxide, and the impact of this oxidative stress on the luminescence properties of the CdSe QDs was studied using steady-state fluorescence, fluorescence lifetime spectroscopy, and ICP-MS. One milliliter of 0.75% hydrogen peroxide was added to 10 mL of 1 μM CdSe QDs in 10 mM phosphate buffer solutions at pH 7.2, and the temporal dependence of the fluorescence spectra (Figure 6A,B) and fluorescence lifetime traces

(Figure 6C,D) were recorded. The fluorescence intensity of both DHLA-PEG750-OCH_3 and BSA-coated QDs decreased over time with a noticeable emission peak blue shift. This is attributed to the oxidation of the QDs, which was previously shown to decrease their size and therefore, to increase their bandgap energy.[35] The fluorescence lifetime of both types of CdSe QDs decreased sharply as well, from 10.8 ± 0.7 to 3.3 ± 0.4 (Figure 6C) and from 13.6 ± 1.2 to 1.4 ± 0.2 ns (Figure 6D). Similarly to our observations in the thermal degradation studies (Figure 5), the fluorescence lifetime becomes more monoexponential in character as complex radiative transitions give way to nonradiative transitions. The sharp decrease in the QD emission intensity and the fluorescence lifetime indicates rapid QD degradation. We investigated whether the degradation of CdSe QDs under these conditions results in QD dissolution. QDs were filtered out of the observed solutions by centrifugation using 30 K MWCO spin filtration devices, and the ionic content of the remaining filtrates was analyzed using ICP-MS. It should be noted that these are challenging measurements because it is difficult to completely remove the QDs out of the solution. Any remaining nonprecipitated QDs would result in a false positive contribution to the measured ionic content in the filtrates. Our ICP-MS measurements did not reveal a substantial ionic content in the QD filtrates, suggesting that the rate of QD dissolution is rather low under the specific hydrogen peroxide exposures used in our experiments. These results point to surface oxidation, which leads to corresponding decreases in the emission QY and fluorescence lifetime because of the emergence of nonradiative transitions, without affecting QD dissolution, as the main QD degradation mechanism.

SUMMARY AND CONCLUSIONS

This study demonstrates the use of fluorescence lifetime spectroscopy, in combination with other fluorescence and analytical methods, for real-time monitoring of QD formation and degradation in solution. QD fluorescence lifetime measurements respond with high sensitivity to changes in the QD crystalline quality, to changes in the QD size and size distribution, and to changes in the QD chemical environment. Although the QD fluorescence lifetime decays are rich in information content, simultaneous changes in the QD size, size distribution, and degradation state could impact the fluorescence lifetime in opposite directions and lead to confusing results if fluorescence lifetime spectroscopy is used as a stand-alone technique and without adequately controlling the experimental variables. It is extremely important to maintain all variables but one constant, if possible, to obtain meaningful and interpretable results. Additionally, our study makes use of the weighted average QD fluorescence lifetime and deviations of the QD fluorescence lifetime from the monoexponential character to provide detailed information about the formation and degradation of luminescent QDs in solution. The QD weighted average fluorescence lifetime and the deviation of the fluorescence lifetime from the monoexponential decay fit function are convenient and suitable means to monitor the interactions of luminescent QDs with the environment as they form or degrade, but are of limited utility in describing the complex photodynamical properties and mechanisms of luminescent QDs. Such studies require a low temperature, time-resolved, and single QD luminescence measurements. Nevertheless, the use of the weighted average fluorescence lifetime, and the deviation of the QD fluorescence lifetime from monoexponential decay, simplifies the analysis and provides important

insights into the interactions between the luminescent QDs and their environment as they form and degrade. The study reveals numerous scenarios where adding fluorescence lifetime spectroscopy of luminescent QDs to the existing tool kit of analytical techniques either corroborate and/or add new information about the QD properties that could inform their synthesis and the parameters that affect their chemical degradation under environmental conditions. For example, fluorescence lifetime spectroscopy measurements reveal with great sensitivity the impact of various reaction methods used to form the QDs on their luminescence properties. Fluorescence lifetime measurements corroborate the emission QY and emission peak width measurements, which show that passivating the CdSe QDs with a ZnS shell improves their luminescence properties. They also clearly show that most of the positive impact of QD passivation is realized by forming a single monolayer shell on the QD core surface. This observation might have important implications on applications where QDs are embedded in a polymer film and protected from the environment by a glass shield, for example, in tablets and QD TVs because passivating the QDs with a single monolayer shell would enable product developers to increase the QD density and the overall brightness of QD-containing polymer films. A thicker shell would still be necessary to passivate the QDs that are used for bioimaging and environmental sensing because of the direct interactions of the QDs with water and other small biomolecules that are ubiquitous in the environment. Fluorescence lifetime spectroscopy studies agree with steady-state fluorescence measurements that show that CdSe QDs dissolved in chloroform degrade rapidly under conditions of elevated temperature. The sharp decrease in the fluorescence lifetime indicates that the chemical degradation of the QDs provides nonradiative pathways to electrons that are slow to undergo radiative electron–hole recombination processes. This raises a concern about the stability of luminescent QDs under conditions that are typical in solar cells or even in consumer electronic products such as cell phones and light emitting displays and points to the necessity for efficient heat dissipation in QD-containing devices to ensure their long-term stability and performance. Fluorescence lifetime spectroscopy in conjunction with steady-state fluorescence also reveal that the CdSe QDs degrade rapidly under conditions of oxidative stress regardless of whether they are covalently modified with hydrophilic molecular ligands or wrapped with protein molecules. ICP-MS of QD filtrates does not show a significant level of dissolution. We therefore conclude that the surface oxidation is likely to be the dominant QD degradation mechanism under the specific oxidative stress conditions in our study.

In summary, the study shows that adding fluorescence lifetime spectroscopy to the tool kit of techniques used to study the formation and degradation of luminescent QDs in solution provides new quantitative real-time information about the QD luminescence properties as they grow and degrade. The study also points to the limitations of fluorescence lifetime spectroscopy, and by extension of fluorescence lifetime imaging of luminescent QD, particularly as a stand-alone technique. It is fair to conclude that combining fluorescence lifetime measurements with emission QY, peak shape and width measurements, and with other analytical methods such as UV–Vis, TEM, and ICP-MS is necessary to provide real-time information about the formation and degradation of core and core/shell QDs in solution under environmentally relevant conditions.

Supplementary Material

Refer to Web version on PubMed Central for supplementary material.

ACKNOWLEDGMENTS

This study was supported by NSF award CHE-1506995. TEM measurements were performed at the National Institute of Standards and Technology (NIST) Center for Nanoscale Science and Technology. The authors thank Dr. Alline Myers of NIST for her assistance with TEM imaging and Drs. Kimihiro Susumu and Igor Medintz of the U. S. Naval Research Laboratory for their assistance in the QD synthesis.

REFERENCES

(1). Alivisatos AP Semiconductor Clusters, Nanocrystals, and Quantum Dots. Science 1996, 271, 933–937.

(2). Bruchez M; Moronne M; Gin P; Weiss S; Alivisatos AP Semiconductor Nanocrystals as Fluorescent Biological Labels. Science 1998, 281, 2013–2016. [PubMed: 9748157]

(3). Steigerwald ML; Alivisatos AP; Gibson JM; Harris TD; Kortan R; Muller AJ; Thayer AM; Duncan TM; Douglass DC; Brus LE Surface Derivatization and Isolation of Semiconductor Cluster Molecules. J. Am. Chem. Soc 1988, 110, 3046–3050.

(4). Brennan JG; Siegrist T; Carroll PJ; Stuczynski SM; Brus LE; Steigerwald ML The Preparation of Large Semiconductor Clusters Via the Pyrolysis of a Molecular Precursor. J. Am. Chem. Soc 1989, 111, 4141–4143.

(5). Murray CB; Norris DJ; Bawendi MG Synthesis and Characterization of Nearly Monodisperse CdE (E = Sulfur, Selenium, Tellurium) Semiconductor Nanocrystallites. J. Am. Chem. Soc 1993, 115, 8706–8715.

(6). Greytak AB; Allen PM; Liu W; Zhao J; Young ER; Popović Z; Walker BJ; Nocera DG; Bawendi MG Alternating Layer Addition Approach to CdSe/CdS Core/Shell Quantum Dots with Near-Unity Quantum Yield and High On-Time Fractions. Chem. Sci 2012, 3, 2028–2034. [PubMed: 24932403]

(7). Nozik AJ; Beard MC; Luther JM; Law M; Ellingson RJ; Johnson JC Semiconductor Quantum Dots and Quantum Dot Arrays and Applications of Multiple Exciton Generation to Third-Generation Photovoltaic Solar Cells. Chem. Rev 2010, 110, 6873–6890. [PubMed: 20945911]

(8). Singh S; Nalwa HS Nanotechnology and Health Safety—Toxicity and Risk Assessments of Nanostructured Materials on Human Health. J. Nanosci. Nanotechnol 2007, 7, 3048–3070. [PubMed: 18019130]

(9). Grecco HE; Lidke KA; Heintzmann R; Lidke DS; Spagnuolo C; Martinez OE; Jares-Erijman EA; Jovin TM Ensemble and Single Particle Photophysical Properties (Two-Photon Excitation, Anisotropy, FRET, Lifetime, Spectral Conversion) of Commercial Quantum Dots in Solution and in Live Cells. Microsc. Res. Tech 2004, 65, 169–179. [PubMed: 15630694]

(10). Carlini L; Nadeau JL Uptake and Processing of Semiconductor Quantum Dots in Living Cells Studied by Fluorescence Lifetime Imaging Microscopy (FLIM). Chem. Commun 2013, 49, 1714–1716.

(11). Liang X; Grice JE; Zhu Y; Liu D; Sanchez WY; Li Z; Crawford DHG; Le Couteur DG; Cogger VC; Liu X; Xu ZP; Roberts MS Intravital Multiphoton Imaging of the Selective Uptake of Water-Dispersible Quantum Dots into Sinusoidal Liver Cells. Small 2015, 11, 1711–1720. [PubMed: 25504510]

(12). Schlegel G; Bohnenberger J; Potapova I; Mews A Fluorescence Decay Time of Single Semiconductor Nanocrystals. Phys. Rev. Lett 2002, 88, 137401. [PubMed: 11955124]

(13). Kethineedi VR; Crivat G; Tarr MA; Rosenzweig Z Quantum Dot-NBD-Liposome Luminescent Probes for Monitoring Phospholipase A2 Activity. Anal. Bioanal. Chem 2013, 405, 9729–9737. [PubMed: 24173659]

(14). Quach AD; Crivat G; Tarr MA; Rosenzweig Z Gold Nanoparticle–Quantum Dot–Polystyrene Microspheres as Fluorescence Resonance Energy Transfer Probes for Bioassays. J. Am. Chem. Soc 2011, 133, 2028–2030. [PubMed: 21280652]

(15). Crivat G; Da Silva SM; Reyes DR; Locascio LE; Gaitan M; Rosenzweig N; Rosenzweig Z Quantum Dot FRET-Based Probes in Thin Films Grown in Microfluidic Channels. J. Am. Chem. Soc 2010, 132, 1460–1461. [PubMed: 20073459]

(16). Shi L; Rosenzweig N; Rosenzweig Z Quantum Dot Based Probes for Screening Proteases and Protease Inhibitors. Anal. Chem 2006, 78, 5799–5804. [PubMed: 16906726]

(17). Shi L; de Paoli V; Rosenzweig N; Rosenzweig Z Synthesis and Application of Quantum Dots FRET-Based Protease Sensors. J. Am. Chem. Soc 2006, 128, 10378–10379. [PubMed: 16895398]

(18). Blagoi G; Rosenzweig N; Rosenzweig Z Design, Synthesis, and Application of Particle-Based Fluorescence Resonance Energy Transfer Sensors for Carbohydrates and Glycoproteins. Anal. Chem 2005, 77, 393–399. [PubMed: 15649033]

(19). Kamat PV; Scholes GD Quantum Dots Continue to Shine Brightly. J. Phys. Chem. Lett 2016, 7, 584–585. [PubMed: 26842359]

(20). Zhao K; Pan Z; Zhong X Charge Recombination Control for High Efficiency Quantum Dot Sensitized Solar Cells. J. Phys. Chem. Lett 2016, 7, 406–417. [PubMed: 26758605]

(21). Furdyna JK; Lee S; Daruka I Self-Assembled Growth of II–VI Quantum Dots. MCLC S&T, Sect. B: Nonlinear Opt 1997, 18, 85–92.

(22). Lee J; Tsakalakos T Influences of Growth Conditions on Physical, Optical Properties, and Quantum Size Effects of CdS Nanocluster Thin Films. Nanostruct. Mater 1997, 8, 381–398.

(23). Zhang BP; Yasuda T; Isoya G; Wang WX; Segawa Y; Edamatsu K; Itoh T Micro-photoluminescence of ZnCdSe quantum dots formed under selected growth conditions. MCLC S&T, Sect. B: Nonlinear Opt 1997, 18, 303–306.

(24). Kalita M; Cingarapu S; Roy S; Park SC; Higgins D; Jankowiak R; Chikan V; Klabunde KJ; Bossmann SH Direct Synthesis of Aqueous Quantum Dots through 4,4′-Bipyridine-Based Twin Ligand Strategy. Inorg. Chem 2012, 51, 4521–4526. [PubMed: 22443511]

(25). Zhang Y; Mi L; Wang P-N; Ma J; Chen J-Y pH-dependent aggregation and photoluminescence behavior of thiol-capped CdTe quantum dots in aqueous solutions. J. Lumin 2008, 128, 1948–1951.

(26). Medintz IL; Uyeda HT; Goldman ER; Mattoussi H Quantum dot bioconjugates for imaging, labelling and sensing. Nat. Mater 2005, 4, 435–446. [PubMed: 15928695]

(27). Chen L-N; Wang J; Li W-T; Han H-Y Aqueous one-pot synthesis of bright and ultrasmall CdTe/CdS near-infrared-emitting quantum dots and their application for tumor targeting in vivo. Chem. Commun 2012, 48, 4971–4973.

(28). van Embden J; Jasieniak J; Mulvaney P Mapping the Optical Properties of CdSe/CdS Heterostructure Nanocrystals: The Effects of Core Size and Shell Thickness. J. Am. Chem. Soc 2009, 131, 14299–14309. [PubMed: 19754114]

(29). Jasieniak J; Smith L; van Embden J; Mulvaney P; Califano M Re-Examination of the Size-Dependent Absorption Properties of CdSe Quantum Dots. J. Phys. Chem. C 2009, 113, 19468–19474.

(30). Xie R; Kolb U; Li J; Basché T; Mews A Synthesis and Characterization of Highly Luminescent CdSe–Core CdS/Zn0.5Cd0.5S/ZnS Multishell Nanocrystals. J. Am. Chem. Soc 2005, 127, 7480–7488. [PubMed: 15898798]

(31). Mei BC; Susumu K; Medintz IL; Mattoussi H Polyethylene glycol-based bidentate ligands to enhance quantum dot and gold nanoparticle stability in biological media. Nat. Protoc 2009, 4, 412–423. [PubMed: 19265800]

(32). Mei BC; Susumu K; Medintz IL; Delehanty JB; Mountziaris TJ; Mattoussi H Modular poly(ethylene glycol) ligands for biocompatible semiconductor and gold nanocrystals with extended pH and ionic stability. J. Mater. Chem 2008, 18, 4949–4958.

(33). Liu D; Snee PT Water-Soluble Semiconductor Nanocrystals Cap Exchanged with Metalated Ligands. ACS Nano 2011, 5, 546–550. [PubMed: 21141814]

(34). Rabouw FT; Kamp M; van Dijk-Moes RJA; Gamelin DR; Koenderink AF; Meijerink A; Vanmaekelbergh D Delayed Exciton Emission and Its Relation to Blinking in CdSe Quantum Dots. Nano Lett 2015, 15, 7718–7725. [PubMed: 26496661]

(35). Ihly R; Tolentino J; Liu Y; Gibbs M; Law M The Photothermal Stability of PbS Quantum Dot Solids. ACS Nano 2011, 5, 8175–8186. [PubMed: 21888407]

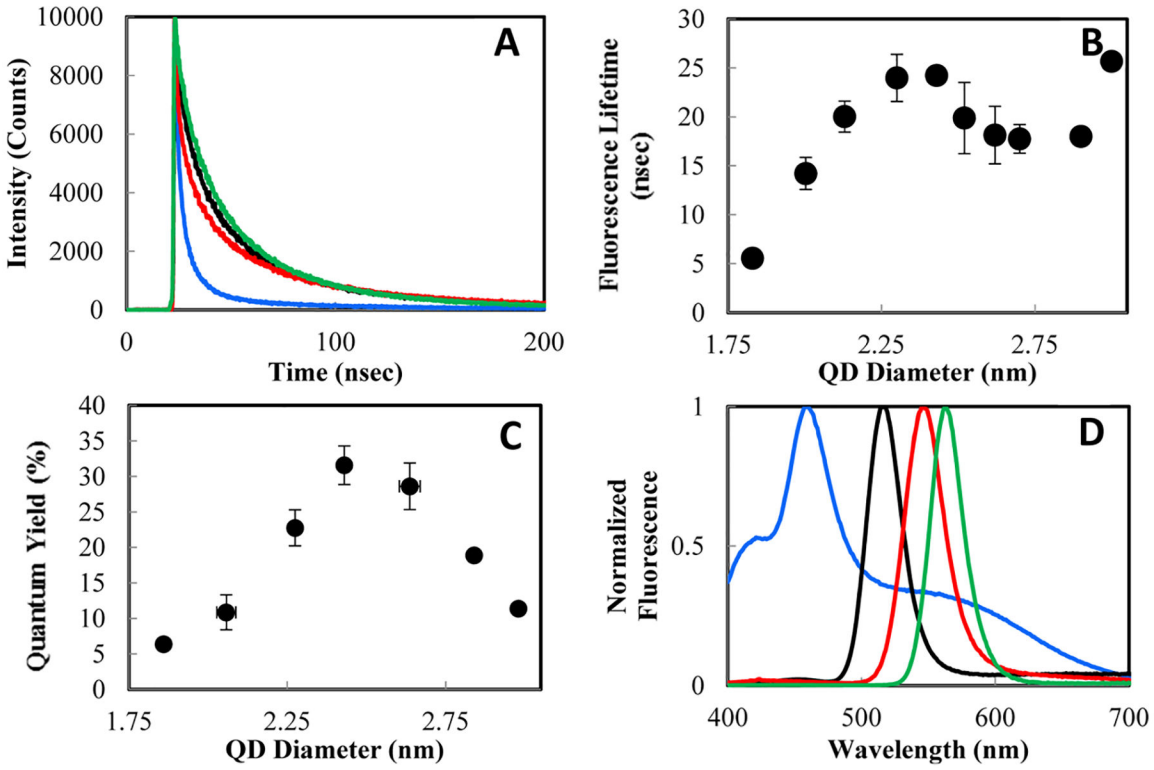

Figure 1.

(A) Fluorescence lifetime traces of CdSe QDs of increasing diameter prepared using a rapid synthesis method [1.8 nm (blue), 2.4 nm (black), 2.9 nm (red), and 3.2 nm (green)], (B) complex size dependence of QD fluorescence lifetime, (C) size dependence of the QD emission QY, and (D) steady-state fluorescence spectra of QDs of increasing diameter. All measurements were taken after the QD cores were purified and suspended in chloroform at room temperature.

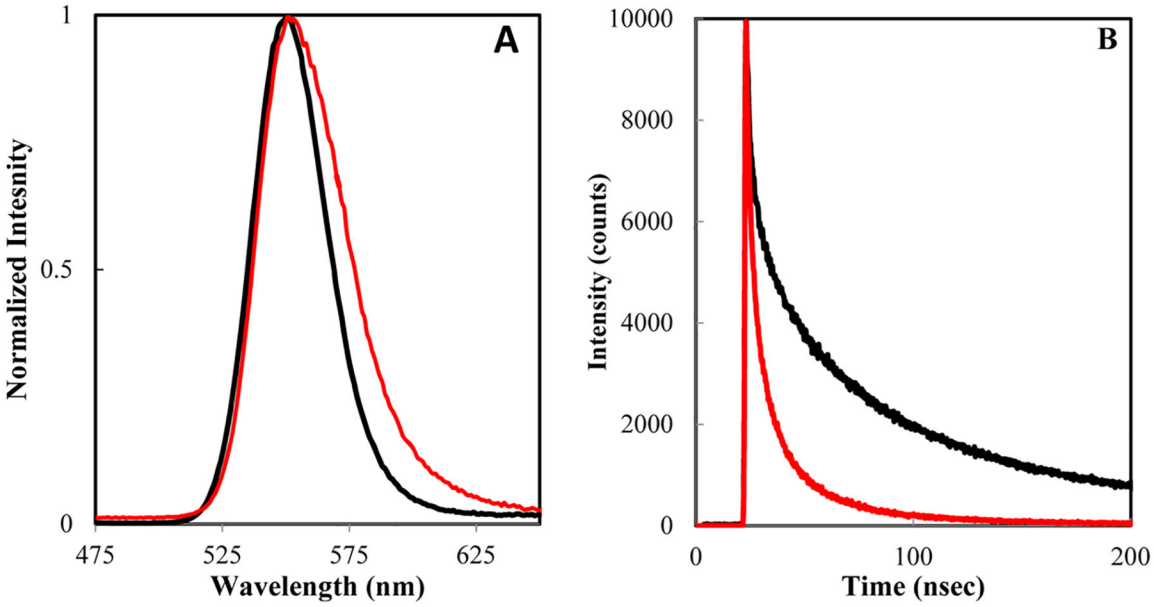

Figure 2.

(A) Normalized steady-state fluorescence spectra of 3.2 nm CdSe QDs synthesized using the “rapid” (red) and “slow” (black) synthesis techniques and (B) corresponding fluorescence lifetime traces. The excitation wavelength was 375 nm and the fluorescence lifetime traces were measured at the emission peak intensity of 555 nm. All measurements were taken after the CdSe QDs were purified and suspended in chloroform at room temperature.

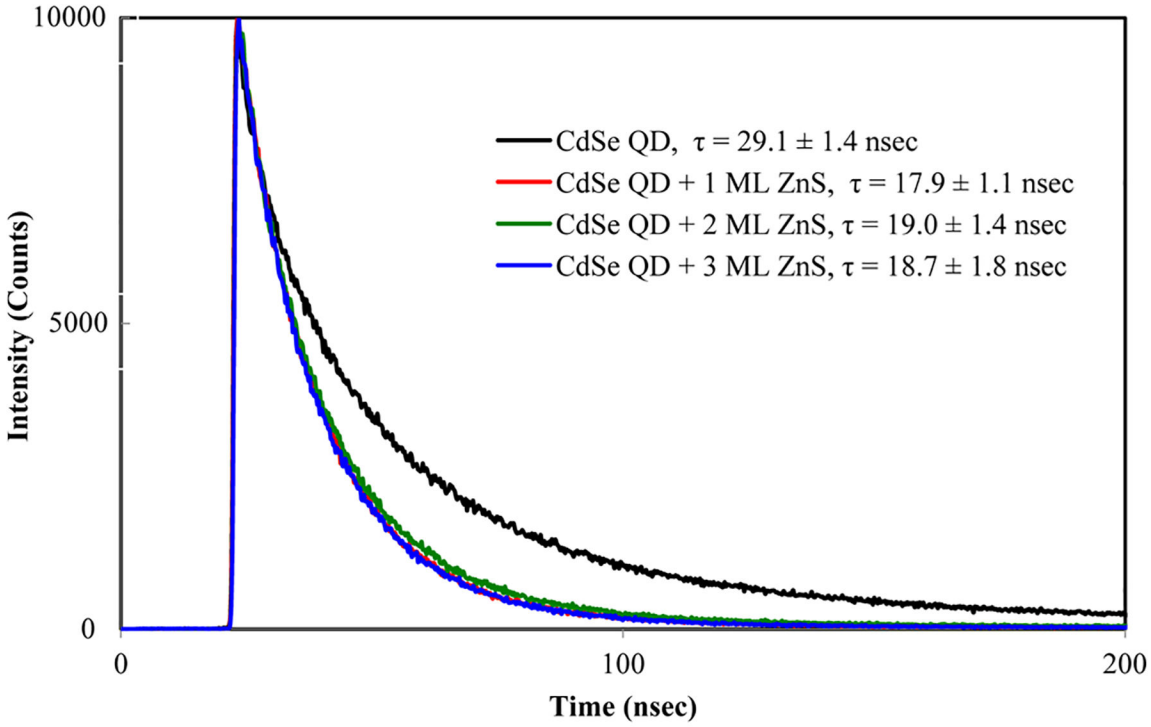

Figure 3.

Fluorescence lifetime traces of 3.0 nm CdSe QDs when they are capped monolayer by monolayer with a ZnS shell using the SILAR method. The excitation wavelength was 375 nm. Fluorescence lifetime traces were measured at the maximum emission peak intensities of 530 nm (CdSe QDs), 560 nm (CdSe QDs with one monolayer ZnS shell), 570 nm (CdSe QDs with two monolayers ZnS shell), and 575 nm (CdSe QDs with three monolayers ZnS shell). CdSe and CdSe/ZnS QDs were purified and suspended in chloroform at room temperature.

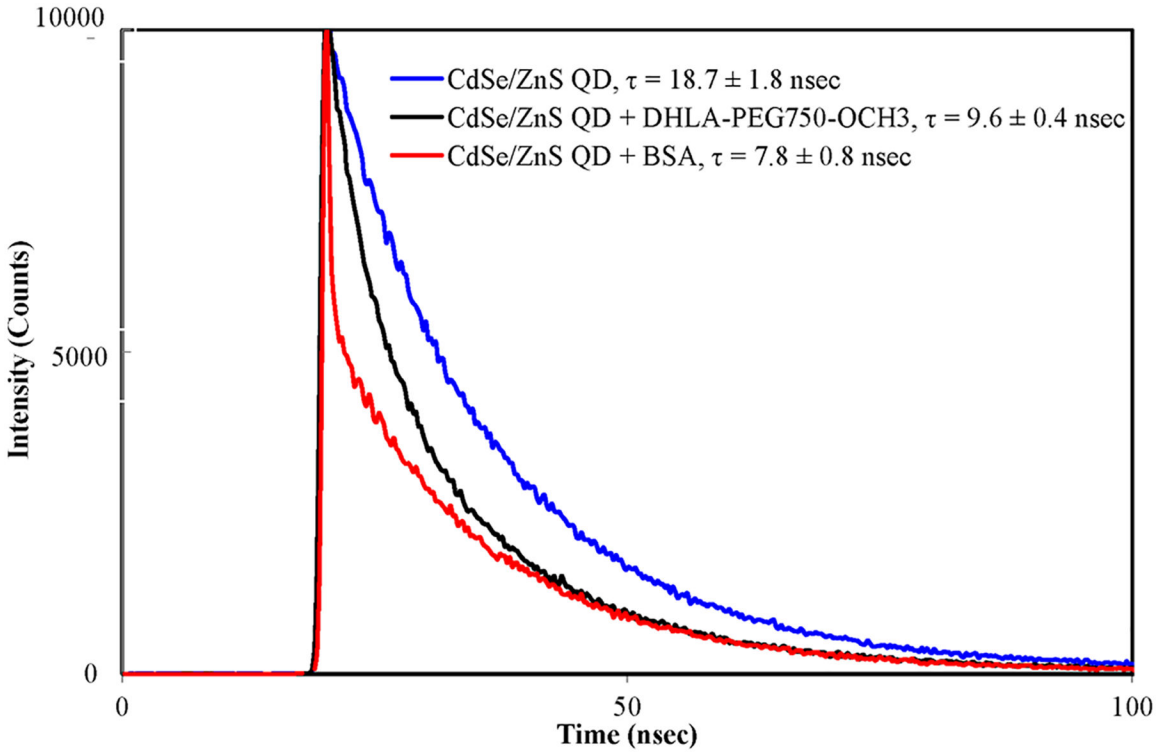

Figure 4.

Fluorescence lifetime traces of CdSe/ZnS QDs (2.4 nm CdSe QD with three monolayers ZnS shell) capped with TOPO (blue) in chloroform, with DHLA-PEG750-OCH3 molecular ligands (black) and with BSA (red) in 10 mM phosphate buffer solution at pH 7.4. The excitation wavelength was 375 nm, and the fluorescence lifetime traces were measured at 570 nm for all samples.

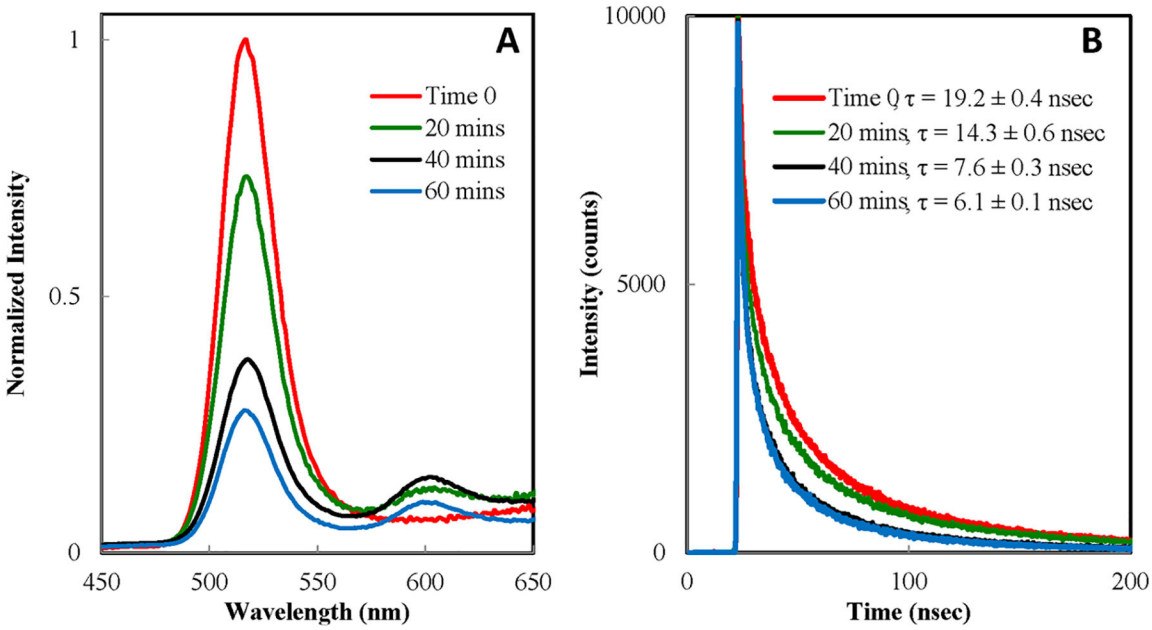

Figure 5.

Fluorescence spectra (A) and fluorescence lifetime traces (B) of 2.4 nm CdSe QDs in chloroform under conditions of elevated temperature of 60 °C for 60 min. The excitation wavelength was 375 nm. The fluorescence lifetime was measured at the QD emission peak wavelength of 530 nm. The decrease in both fluorescence intensity without a noticeable peak shift and fluorescence lifetime over time indicates QD degradation without a significant change in the QD size under conditions of elevated temperature.

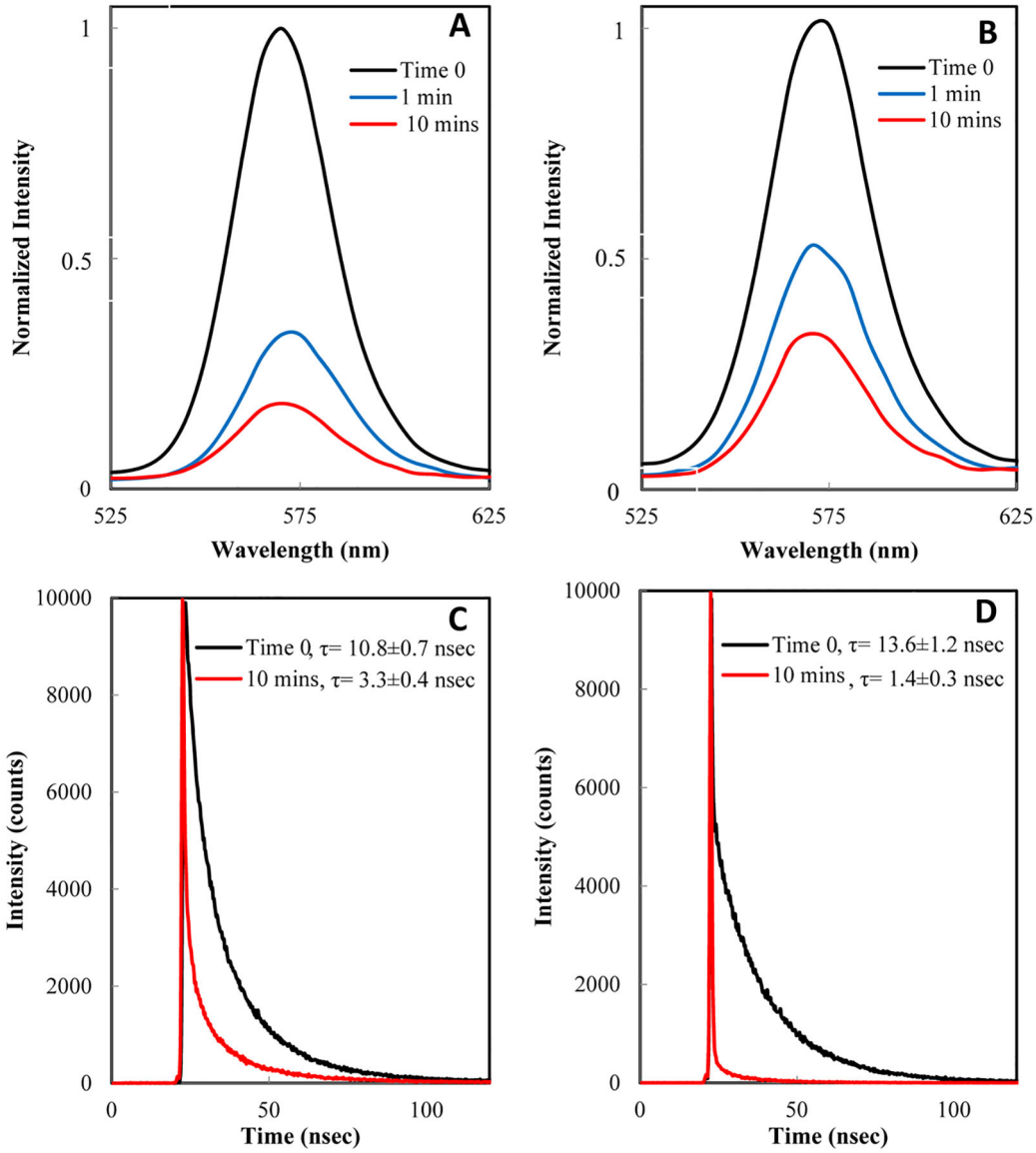

Figure 6.

Steady-state fluorescence (A,B) and fluorescence lifetime traces (C,D) of CdSe QDs capped with DHLA-PEG (A,C) and BSA (B,D) in 10 mM phosphate buffer at pH 7.4, when hydrogen peroxide solution is added to a final concentration of 0.75%. The excitation wavelength was 375 nm. The fluorescence lifetime was measured at the QD emission peak intensity of 530 nm. The decrease in both fluorescence intensity with a noticeable peak blue shift and fluorescence lifetime indicates QD degradation under conditions of oxidative stress.